The EMBO Journal Vol.18 No.19 pp.5285–5299, 1999

Initiation of IP_3-mediated Ca^{2+} waves in *Xenopus* oocytes

Jonathan Marchant, Nick Callamaras and Ian Parker[1]

Laboratory of Cellular and Molecular Neurobiology, Department of Neurobiology and Behavior, University of California, Irvine, CA 92697-4550, USA

[1]Corresponding author
e-mail: iparker@uci.edu

Inositol (1,4,5)-trisphosphate (IP_3) evokes Ca^{2+} liberation in *Xenopus* oocytes as elementary events (Ca^{2+} puffs) that become coupled to propagate Ca^{2+} waves with increasing [IP_3]. To investigate this transition between local and global Ca^{2+} signaling, we developed an optical method for evoking rapid subcellular Ca^{2+} elevations, while independently photoreleasing IP_3 and simultaneously recording confocal Ca^{2+} images. Focal Ca^{2+} elevations triggered waves within 100 ms of photoreleasing IP_3, compared with latencies of seconds following photorelease of IP_3 alone. Wave velocity varied with [IP_3] but was independent of time after photorelease of IP_3, indicating that delayed wave initiation did not involve slow binding of IP_3 to its receptors. The amount of Ca^{2+} required to trigger a wave was ~10-fold greater than the average size of puffs, and puffs showed no progressive increase in magnitude before waves initiated. Instead, Ca^{2+} puffs contributed to a slow rise in basal free [Ca^{2+}], which further increased puff frequency and sensitized IP_3 receptors so that individual events then triggered waves. Because the wave threshold is much greater than the size of the elementary puff, cells can employ both local and global signaling mechanisms, and the summation of stochastic behavior of elementary events allows generation of reproducible periodic waves.

Keywords: Ca^{2+} puffs/Ca^{2+} waves/inositol trisphosphate/*Xenopus* oocytes

Introduction

In numerous cell types, activation of the inositol (1,4,5)-trisphosphate (IP_3) second messenger pathway generates periodic oscillations in the concentration of cytoplasmic Ca^{2+} ($[Ca^{2+}]_{cyt}$), manifested as repetitive Ca^{2+} waves that propagate throughout the cell (Berridge and Dupont, 1994; Thomas *et al.*, 1996). These macroscopic Ca^{2+} signals regulate cellular functions through both frequency- and amplitude-dependent mechanisms (Gu and Spitzer, 1995; Berridge, 1997a; Dolmetsch *et al.*, 1997; Li *et al.*, 1998). The complex spatiotemporal patterns of Ca^{2+} release depend on the functional properties and subcellular localization of endogenous IP_3 receptors. It is well established that the stimulatory and inhibitory effects of cytosolic Ca^{2+} on IP_3 receptor activity (Iino, 1990; Parker and Ivorra, 1990; Bezprozvanny *et al.*, 1991; Finch *et al.*, 1991; Marshall and Taylor, 1993; Horne and Meyer, 1995; Hagar *et al.*, 1998; Ramos-Franco *et al.*, 1998), together with the positively cooperative nature of IP_3-stimulated Ca^{2+} release (Meyer *et al.*, 1990; Marchant and Taylor, 1997) are crucial in establishing patterns of Ca^{2+} spiking. Furthermore, high-resolution confocal imaging techniques have revealed that IP_3-sensitive Ca^{2+} release occurs in various cell types at discrete, subcellular sites, formed by clusters of probably a few tens of active IP_3 receptors (Parker and Yao, 1991; Bootman and Berridge, 1995; Parker *et al.*, 1996a; Berridge, 1997b; Horne and Meyer, 1997). At low concentrations of IP_3, these individual release units function autonomously, generating transient, localized release events termed 'Ca^{2+} puffs' (Parker and Yao, 1991; Yao *et al.*, 1995; Bootman *et al.*, 1997a,b; Sun *et al.*, 1998). Higher concentrations of IP_3 sufficiently sensitize neighboring Ca^{2+} release sites so that the cytoplasm acts as an excitable medium through which Ca^{2+} waves propagate in a saltatory manner in successive rounds of Ca^{2+}-induced Ca^{2+} release (CICR) and Ca^{2+} diffusion (Parker *et al.*, 1996a; Berridge, 1997b; Bootman *et al.*, 1997b; Callamaras *et al.*, 1998).

Applications of Ca^{2+}-mobilizing agonists evoke global cellular Ca^{2+} signals, which arise following dose-dependent latencies that can be as long as many seconds or minutes at just-suprathreshold agonist concentrations (Miledi and Parker, 1989; Berridge, 1994). Part of this delay arises from the slow build-up of IP_3, yet dose-dependent latencies of several seconds or longer are still apparent when cytosolic [IP_3] is elevated almost instantly by photorelease from a caged precursor (Parker *et al.*, 1996b; Callamaras *et al.*, 1998). Prior to the initiation of global Ca^{2+} waves, local elementary Ca^{2+} signals are observed, which probably serve as triggers for Ca^{2+} waves that subsequently propagate by successive cycles of Ca^{2+} diffusion and CICR at discrete IP_3-sensitive release sites (Parker and Yao, 1991; Bootman *et al.*, 1997a,b; Callamaras *et al.*, 1998). As well as serving as the 'building blocks' from which global signals are initiated and propagated, the elementary Ca^{2+} events may also permit a targeted and economic delivery of Ca^{2+} to specific effector systems localized near the release sites (Rizzuto *et al.*, 1993; Nelson *et al.*, 1995; Berridge *et al.*, 1998). Whereas Ca^{2+} waves synchronize cellular responses, localized Ca^{2+} signaling allows for asynchronous regulation of functionally discrete compartments. Indeed, independent functions have been ascribed to localized and global Ca^{2+} signals in various cell types (Nelson *et al.*, 1995; Thorn, 1996), most notably the differential regulation of tone by Ca^{2+} sparks and waves in arterial smooth muscle (Nelson *et al.*, 1995). An understanding of the mechanisms underlying the transition from elementary Ca^{2+} puffs to waves is thus of crucial functional importance.

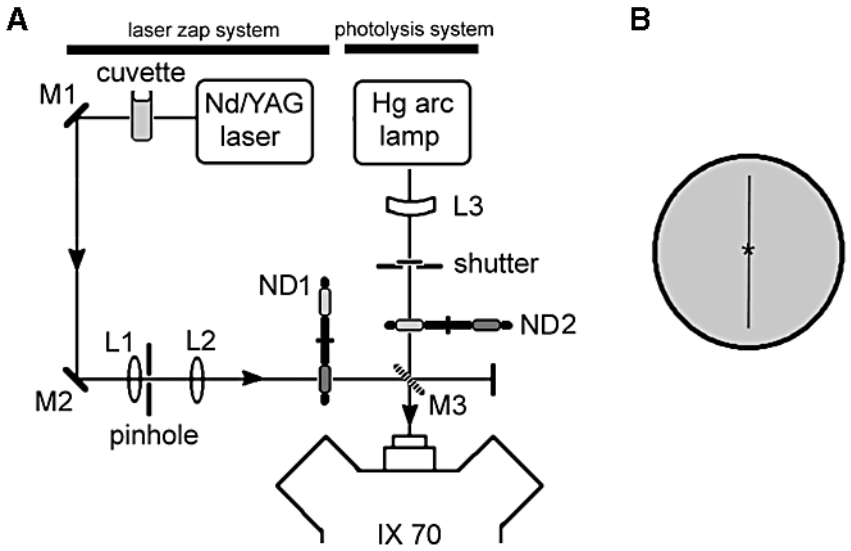

Fig. 1. Optical system for photostimulation. (**A**) Schematic diagram of the systems for wide-area photolysis of caged IP_3 and localized photodamage (laser 'zap'). Photolysis light was derived from a continuous 100 W Hg arc lamp, using an electronically controlled shutter to set the flash duration, and neutral density wheels (ND2) to vary the intensity. The laser zap system generated pulses (λ = 355 nm, ~5 ns duration) from a frequency-tripled Nd–YAG laser, which were directed through a separate optical path to generate local intracellular Ca^{2+} transients resulting from localized photodamage in the oocyte. Light from both optical paths was combined by a 50/50 partially silvered mirror (M3) and directed through the epifluorescence port into an Olympus IX70 inverted microscope fitted with a standard UV fluorescence cube. The UV laser beam was first attenuated to ~10% by passage through a cuvette filled with a solution of $FeSO_4$, as the unattenuated beam otherwise was sufficiently strong to damage coatings on mirrors in the light path. Mirrors M1 and M2 directed the laser light through a spatial filter/beam expander formed by lenses L1 (10× fluorescence microscope objective) and L2 (fused silica converging singlet, f = 10 cm) and a 100-μm pinhole. This was used both to improve the beam quality and to fill the back aperture of the microscope objective lens (40× oil-immersion; numerical aperture = 1.35), thereby allowing the beam to be focused to a spot of ~1 μm diameter in the specimen plane of the microscope. A separate neutral density wheel (ND1) allowed control of the beam intensity independently of the UV photolysis light. The laser was triggered by a TTL pulse at set times during the recording cycle. Confocal linescan images were obtained by a separate scanning system interfaced through the side port of the microscope (not shown; for details see Parker *et al.*, 1997). (**B**) Arrangement of confocal linescan, UV photolysis light and laser zap spot in the oocyte. The vertical line represents the 100-μm confocal scan line. The UV photolysis light was focused concentrically around the scan line, throughout a uniform circular area of ~150 μm diameter (gray circle). The laser zap spot was positioned in the center of the scan line (*), and was confocal with the imaging laser line.

A key element in the generation of local and global Ca^{2+} signals involves the dual roles of Ca^{2+} and IP_3 ions acting as co-agonists at the IP_3 receptor to determine the excitability of the cytoplasm. However, experimental studies in intact cells have been hampered by the difficulty of independently evoking rapid and reproducible step changes in $[IP_3]_{cyt}$ and $[Ca^{2+}]_{cyt}$. Although the use of caged compounds provides an excellent means of regulating intracellular levels of either IP_3 or Ca^{2+} (Walker *et al.*, 1987; Adams *et al.*, 1988; Kaplan and Ellis-Davies, 1988), it has not been possible to use both compounds simultaneously because of their overlapping excitation wavelengths. Thus, our understanding of the kinetic behavior of IP_3 receptor derives predominantly from studies employing broken cell systems, in which the spatial organization of Ca^{2+} signaling is disrupted (Finch *et al.*, 1991; Combettes *et al.*, 1994; Horne and Meyer, 1995; Dufour *et al.*, 1997; Marchant and Taylor, 1997, 1998).

In the present study, we examined the interrelationship between IP_3 receptor excitability, Ca^{2+} puffs and Ca^{2+} wave initiation in *Xenopus* oocytes, using a novel optical method for evoking rapid local Ca^{2+} elevations in an intact cell, which could be used simultaneously with independent photolytic release of IP_3. Our results show that following moderate, physiologically relevant elevations in cytosolic $[IP_3]$ the cytoplasm became almost immediately capable of supporting Ca^{2+} wave propagation, but that the triggering of waves involves appreciably greater amounts of Ca^{2+} than were liberated during individual puffs. Instead, Ca^{2+} liberation by numerous elementary events drove the ambient $[Ca^{2+}]_{cyt}$ toward a threshold at which a regenerative Ca^{2+} wave was evoked. The positioning of the size of the elementary Ca^{2+} release event well below the threshold for wave initiation allows the cell to use both local and global Ca^{2+} cell signaling mechanisms, and the triggering of waves by summated activity of numerous puffs ensures that regularly periodic global signals can be generated despite the stochastic behavior of the underlying elementary events.

Results

Ca^{2+} imaging and photostimulation

Experiments were carried out using immature *Xenopus* oocytes, imaged using a linescan confocal microscope to monitor fluorescence of the Ca^{2+} indicator Oregon Green 488 BAPTA 1 (OG-1) along a 100-μm scan line focused at a depth of 3–5 μm below the cell surface. The microscope was equipped with two UV systems for photostimulation (Figure 1A). (i) Light from a mercury arc lamp source (340–400 nm) was focused on the oocyte as a 200 μm diameter spot concentric around the laser scan line (Figure 1B) to allow diffuse photolysis of caged IP_3 loaded into the cell. The flash duration and intensity, and hence extent of photorelease, were regulated by an electronic shutter and neutral density filters. (ii) A separate system was used to focus brief (5 ns) pulses of UV (355 nm) light from a frequency-tripled Nd–YAG laser

down to a near diffraction-limited spot in the specimen, which was aligned on the center of the confocal scan line (Figures 1B and 2A). Delivery of pulses (laser 'zaps') to pigmented oocytes resulted in transient photodamage and rapid, local liberation of Ca^{2+} into the cytosol (Figure 2B). These responses did not involve photorelease of IP_3 by the UV laser pulse, since they were observed in oocytes that were not loaded with caged IP_3 (see below). The Ca^{2+} signals increased markedly in magnitude and spatial spread with increasing intensity of the zap (Figure 2B and C). Weak stimuli evoked small Ca^{2+} signals, comparable in size to endogenous elementary Ca^{2+} puffs (see below), whereas progressively stronger zaps evoked more prolonged and extensive signals, and the strongest pulses resulted in localized morphological damage to the cell (evident as a sustained black stripe in the final image in Figure 2B). Except in the case of very strong zaps, successive pulses delivered at intervals of 60 s to the same site elicited repeated responses (data not shown). To quantify the magnitudes of Ca^{2+} signals evoked by zaps of varying intensities, we estimated the 'Ca^{2+} surface' associated with the Ca^{2+} transients by integrating the fluorescence signal throughout the area over which it was elevated. As shown in Figure 2C, the peak Ca^{2+} liberation increased steeply with increasing intensity of the laser pulse. The laser zap technique thus provided a means to evoke precisely timed Ca^{2+} elevations of variable magnitudes that were localized focally on the laser scan line.

Characteristics of cytosolic Ca^{2+} elevations evoked by laser zap

To determine the mechanisms underlying generation of Ca^{2+} signals by the focused UV laser pulses, we studied responses in oocytes that were loaded only with OG-1 (i.e. in the absence of caged IP_3). Several lines of evidence indicated that these laser zap responses involved Ca^{2+} arising from both intracellular and extracellular sources in response to light absorption by pigment granules in the oocyte. First, responses to weak UV pulses were little changed when extracellular free [Ca^{2+}] was either reduced to very low levels by omitting Ca^{2+} and adding EGTA, or when extracellular free [Ca^{2+}] was elevated to 20 mM (Figure 2D). In contrast, responses to strong zaps increased with increasing extracellular [Ca^{2+}], indicating that Ca^{2+} influx across the plasma membrane was the major source of Ca^{2+} evoked by these more intense stimuli. Secondly, Ca^{2+} responses could not be evoked in oocytes from albino frogs (which lack pigment granules), even with unattenuated laser pulses ~150 times stronger than signals sufficient to evoke responses in pigmented oocytes (Figure 2E, open circles). Finally, the Ca^{2+} signals depended upon the close alignment of the laser spot on a pigment granule. In the vegetal hemisphere of pigmented oocytes, which contains sparsely distributed pigment granules, the average signal with the laser spot focused on granules was ~25-fold greater than when the laser spot was positioned randomly (40 trials in each of three oocytes).

A further important point is that in oocytes loaded with caged IP_3 (5 μM), Ca^{2+} signals could be evoked in pigmented oocytes by laser pulses with intensities well below that needed to photorelease sufficient IP_3 to evoke IP_3-mediated Ca^{2+} liberation. We tested this by comparing Ca^{2+} signals evoked by laser zaps of varying intensities delivered to albino oocytes loaded with 5 μM caged IP_3 and to pigmented oocytes that were not loaded with caged IP_3. In albino oocytes loaded with caged IP_3, zaps of progressively increasing strength evoked Ca^{2+} signals that grew from individual puffs to involve regions tens of micrometers across, contrasting with the lack of responses in albino oocytes without caged IP_3. However, the strength of UV laser pulses needed to evoke detectable Ca^{2+} liberation through photolysis of caged IP_3 in albino oocytes was ~10-fold greater than that needed to evoke comparable Ca^{2+} signals by photodamage in pigmented oocytes (Figure 2E, open and filled squares, respectively). In all subsequent experiments, the caged [IP_3] was decreased to 2 μM to reduce further the photorelease of IP_3 to $<5\%$ of the threshold amount required to evoke Ca^{2+} release.

In summary, these results suggest that intracellular Ca^{2+} release evoked via attenuated UV laser pulses are caused by localized photodamage resulting from light absorption by a pigment granule. The high energy during the brief duration (5 ns) of the focused laser pulse presumably results in intense local heating and consequent permeabilization of adjacent membranes. Responses evoked by weak or moderate pulses were transient, indicating that the membrane 'leak' reseals over several seconds. This ability to evoke rapid focal increases in $[Ca^{2+}]_{cyt}$ while independently regulating photorelease of IP_3 allowed us to investigate the interactions of these two intracellular messengers in Ca^{2+} wave initiation.

Ca^{2+} wave initiation by local elevations in cytoplasmic Ca^{2+}

The overall aim of these experiments was to elucidate the factors underlying the increase in cytoplasmic excitability that leads to Ca^{2+} wave initiation. Following moderate increases of [IP_3], waves do not originate until after a delay of several seconds, even though puffs are observed during this latent period (Figure 3B). We first investigated whether the delay between elevating $[IP_3]_{cyt}$ and the initiation of a Ca^{2+} wave arises because the cytoplasm is incapable of supporting wave propagation during this time, or because the cytoplasm is excitable but puffs are insufficient stimuli to trigger waves. To do this we exploited the ability to elevate [IP_3] and [Ca^{2+}] independently, by recording responses to focal elevations of Ca^{2+} evoked by laser zaps delivered at various intervals after photorelease of IP_3.

In the absence of concomitant liberation of IP_3, Ca^{2+} signals evoked by laser zaps remained localized and, irrespective of the intensity of the laser pulse, never initiated Ca^{2+} waves (Figures 2B and 3A). In contrast, photorelease of low concentrations of IP_3 throughout the recording area evoked spontaneous Ca^{2+} waves (Figure 3B), which began after a latency of several seconds (e.g. 4.20 ± 0.45 s, $n = 5$ for the experiment in Figure 3). Subsequent images (Figure 3C–F) show responses to paired delivery of a laser zap at varying intervals after photorelease of IP_3. In all cases, a Ca^{2+} wave was initiated at the site of the laser spot immediately after a Ca^{2+} pulse was delivered. Once triggered, the Ca^{2+} wave propagated as a circular wave of roughly uniform velocity, giving rise to a 'V'-shaped pattern in the linescan image as the

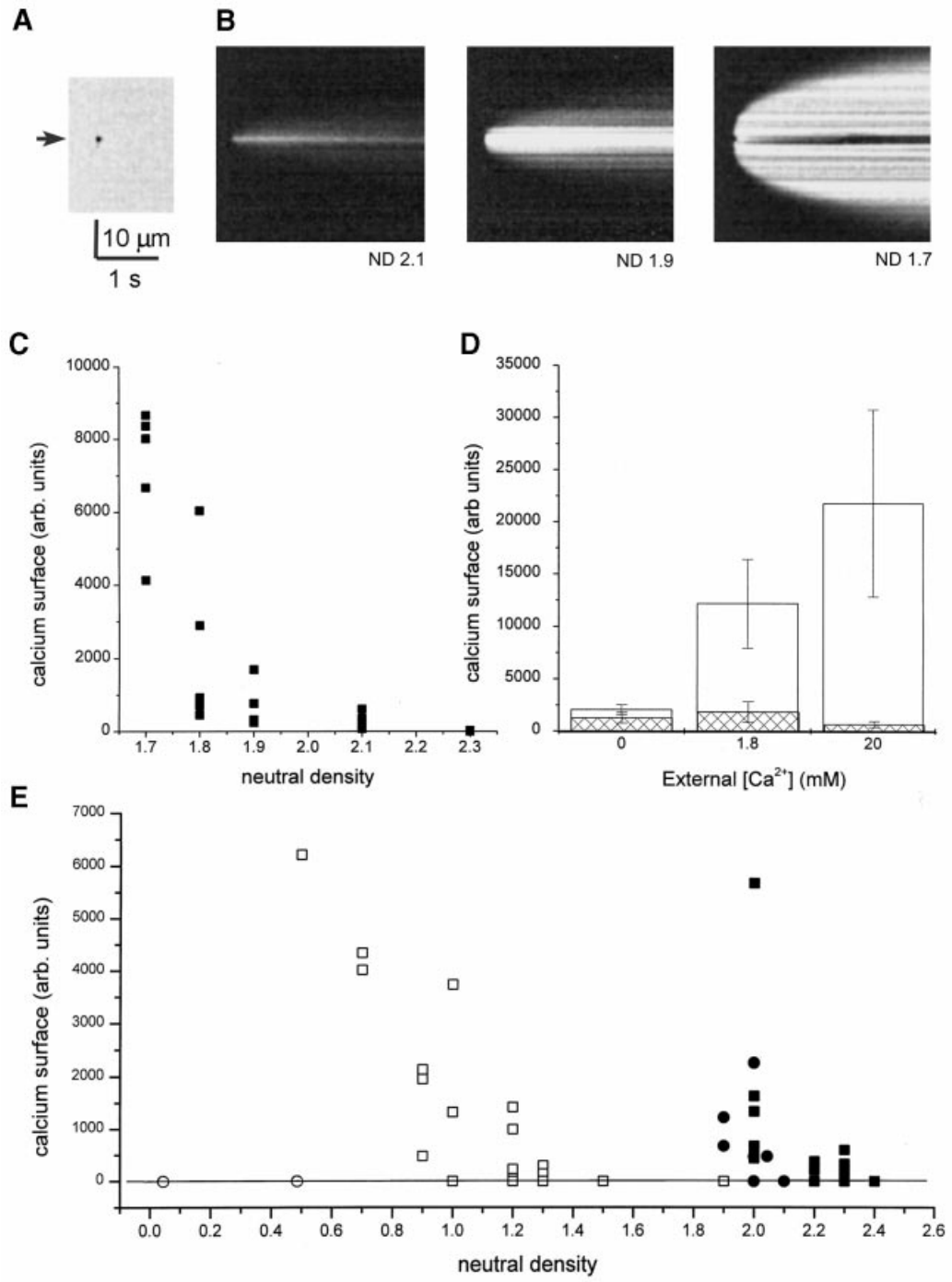

Fig. 2. Characteristics of local Ca^{2+} signals evoked by laser zap. (**A**) Image illustrating the tight focusing of the UV laser zap spot, obtained by bleaching a fluorescent film formed on top of a coverglass using a yellow 'highlighter' pen. The linescan image shows fluorescence along a scan line centered on the UV laser spot (arrow). Induction of the laser zap effect depended strongly on the ability to focus the laser beam to such a small spot in the oocyte, as much higher laser powers were required to evoke Ca^{2+} signals when the spot was deliberately defocused. In this and all other linescan images, time runs from left to right, and distance along the scan line is depicted vertically. (**B**) Linescan images showing Ca^{2+} signals evoked in an oocyte by UV laser pulses of increasing intensity, as indicated by decreasing optical density of the attenuating neutral density filters. In this gray-scale representation, black corresponds to no fluorescence change and white to the maximal fluorescence increase (maximal rise in $[Ca^{2+}]$). Recordings were made in the vegetal hemisphere of a pigmented oocyte, loaded with OG-1. (**C**) Dependence of Ca^{2+} signal on strength of the UV laser pulse. Measurements are expressed as 'Ca^{2+} surface' ($\Delta F/F * \mu m^2$), and are plotted against the degree of attenuation of the UV laser light. Data were obtained from images like those in (B), in three oocytes. (**D**) Ca^{2+} signals evoked by UV laser pulses result from both intracellular Ca^{2+} stores and Ca^{2+} influx. Bars show magnitudes of signals evoked by weak (ND 2.1, hatched bars) and stronger (ND 1.9, open bars) UV laser pulses with oocytes bathed in modified Ringer's solutions containing different free Ca^{2+} concentrations. (**E**) Ca^{2+} signals evoked by UV laser pulses depend on light absorption by pigment granules, and are evoked by laser strengths weaker than those required to photorelease IP_3. Data show magnitudes of Ca^{2+} signals evoked by UV laser pulses of varying intensity under a variety of conditions. Filled symbols indicate measurements from pigmented oocytes, and open symbols derive from albino oocytes. Squares represent data from oocytes injected with both OG-1 and caged IP_3 (final intracellular concentrations ~40 and 5 µM, respectively), whereas oocytes marked by circles were loaded only with OG-1 (40 µM).

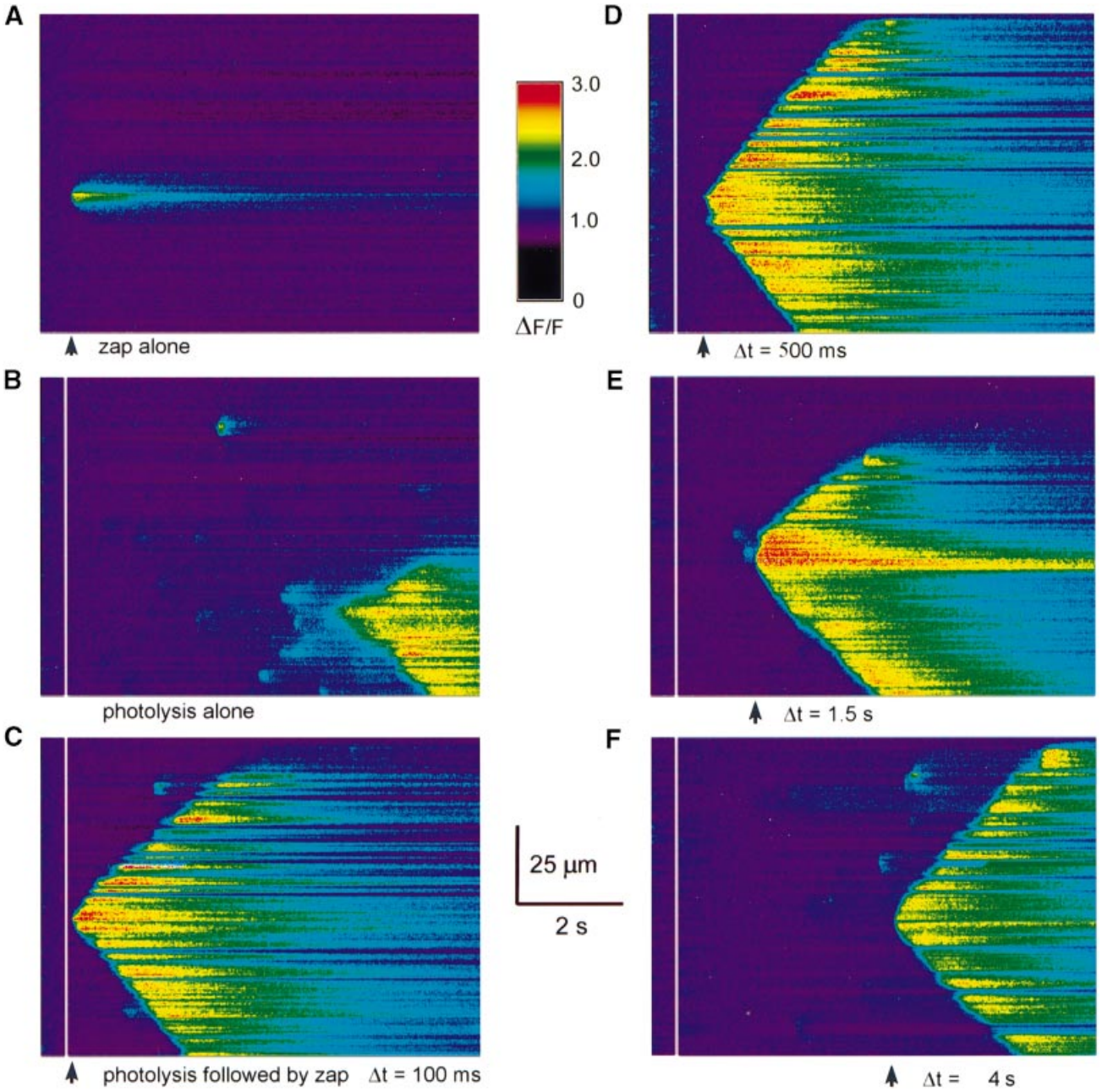

Fig. 3. Local Ca^{2+} elevations can trigger Ca^{2+} waves immediately following photorelease of IP_3. Confocal linescan images depict increasing fluorescence ratios of OG-1 (increasing free $[Ca^{2+}]$) on a pseudocolor scale, as indicated by the color bar. Photolysis flashes of identical intensity and duration (100 ms) were delivered in frames B–F when indicated by white bars. UV laser pulses (all with the same attenuation) were delivered when indicated by the arrows. All records were obtained in a restricted region within the vegetal hemisphere of the same oocyte, and are representative of similar experiments in 23 different oocytes. (**A**) Localized, transient response to a UV laser zap delivered alone, without prior photorelease of IP_3. (**B**) Photorelease of IP_3 alone evoked several Ca^{2+} puffs, followed by a Ca^{2+} wave beginning ~5 s after the photolysis flash. (**C**–**F**) Ca^{2+} waves triggered by UV laser zaps delivered at various intervals (Δt) following photolysis flashes.

wavefronts propagated along the scan line. The striking result was that a Ca^{2+} wave was readily triggered by a Ca^{2+} pulse as soon as 100 ms after moderate photorelease of IP_3 (Figure 3C), despite the fact that spontaneously initiated waves did not occur until after several seconds (Figure 3B). This finding was confirmed in a total of 23 oocytes (seven frogs), indicating that the cytoplasm is capable of supporting wave propagation almost immediately following photorelease of IP_3.

Amount of Ca^{2+} needed to initiate a Ca^{2+} wave

The intensity of the laser zap pulses in Figure 3C–F was adjusted to evoke a Ca^{2+} signal sufficiently large that waves were invariably triggered. Weaker pulses, however, sometimes failed to initiate waves. To quantify the amount of Ca^{2+} needed to trigger a Ca^{2+} wave at a given $[IP_3]_{cyt}$, we determined the probability that zaps of varying strength would initiate waves when delivered at a fixed interval (100 ms) following photorelease of IP_3 concentrations that

evoked spontaneous waves with latencies of ~5 s. Because of the inherent variability in Ca^{2+} signals evoked by zaps of nominally fixed strength (Figure 2), we tested responses to 40 zaps of a given intensity delivered at random locations within the vegetal hemisphere of each oocyte. The first 20 stimuli were delivered after wide-field photolysis of IP_3, so as to estimate the probability that a Ca^{2+} wave would be triggered. The final 20 zaps were delivered without concomitant photolysis of IP_3, to measure the mean amount of Ca^{2+} delivered by each zap. This was estimated by calculating the 'signal mass' associated with the event (Sun *et al.*, 1998). The underlying assumption of this calculation is that, for such focally evoked events, the laser scan line cuts through the center of a symmetrical sphere of Ca^{2+} diffusing from the point source of release. Fluorescence along the scan line thereby represents the profile across the diameter of this sphere such that the total fluorescence change can be computed by integrating the profile throughout three dimensions. The resulting figure is expressed in signal mass units of $\Delta F/F \times 10^{-15}$ l, where one signal mass unit (s.m.u.) corresponds to a doubling of fluorescence throughout a volume of 1 fl (Sun *et al.*, 1998). Under our experimental conditions and using OG-1 as the indicator, 1 s.m.u. corresponds to ~2×10^{-20} mol Ca^{2+} (Sun *et al.*, 1998).

Figure 4A plots the probability of wave initiation as a function of the mean amounts of Ca^{2+} ('signal mass') evoked by laser zaps of varying intensity. Ca^{2+} signals >1000 s.m.u. (~2×10^{-17} mol Ca^{2+}) invariably triggered propagating Ca^{2+} waves. However, as the intensity of the laser zap was reduced to evoke smaller Ca^{2+} signals the probability of wave initiation progressively declined, such that a signal of ~120 s.m.u. (~2.4×10^{-18} mol Ca^{2+}) was effective in triggering a Ca^{2+} wave in only half the trials.

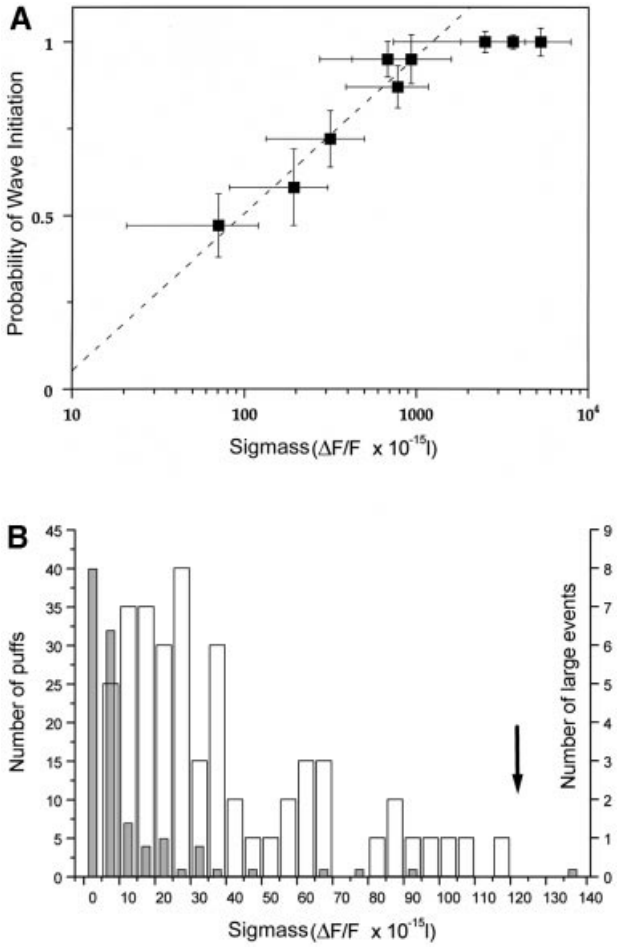

Fig. 4. The amount of Ca^{2+} required to trigger waves is greater than that liberated during puffs. (**A**) Relationship between the amount of Ca^{2+} (expressed as signal mass of OG-1 fluorescence) released by laser zap pulses of varying strengths, and the probability that these transients would trigger a Ca^{2+} wave (see text for details). Data are from five oocytes. (**B**) Histograms show distributions of magnitudes (signal mass), puffs (solid bars) and large events that failed to trigger waves (clear bars). Data are from $n > 5$ oocytes, measured from records like those in Figure 3. Ordinates give numbers of events for puffs (left scale) and large events (right scale). The arrow indicates the signal mass that gave a 50% chance of initiating a wave in the experiment in (A).

Individual puffs are ineffective stimuli for wave initiation

The laser zap experiment described above provides an estimate of how much 'trigger' Ca^{2+} is needed to initiate a Ca^{2+} wave immediately after photorelease of IP_3 at a concentration that, by itself, would evoke a wave only after several seconds. To compare this value with the amount of Ca^{2+} liberated during elementary Ca^{2+} release events, we measured the signal mass associated with Ca^{2+} puffs in the same oocytes (Figure 4B, filled bars). The distribution of the size of Ca^{2+} puffs followed a continuous, roughly exponential distribution (Sun *et al.*, 1998), with an overall mean value of ~17 s.m.u. (~3.4×10^{-19} mol Ca^{2+}). Their mean size was ~7-fold smaller than laser zap responses that had only a 50% chance of initiating a wave (arrow in Figure 4B), and from the exponential distribution of puff magnitudes only ~1.5% of events would be expected to exceed this triggering threshold.

A possible complication in comparing the efficacy of puffs and zap-evoked Ca^{2+} transients to trigger Ca^{2+} waves arises from their different locations in the oocyte. Puffs originate from sites at a mean distance of ~3 μm below the oocyte surface (Callamaras and Parker, 1999), whereas the transients evoked by laser zaps involve Ca^{2+} influx across the plasma membrane (Figure 2D). The radial separation between puff sites and the plasma membrane is, however, comparable to the mean lateral spacing between puff sites in the vegetal hemisphere (2.5 μm; Callamaras and Parker, 1998), so it is likely that a given amount of Ca^{2+} arising from a puff or a laser zap will have a similar probability of triggering CICR at neighboring release sites.

Two further observations also support the notion that individual puffs are generally too small to trigger waves. First, several discrete Ca^{2+} puffs were usually observed preceding Ca^{2+} waves in typical linescan images (e.g. Figure 3B), but they failed to act as foci for wave initiation even though the cytoplasm was sufficiently excitable to support wave propagation (Figure 3C). For example, in seven records like that in Figure 3B, a mean of 5.85 (± 1.2) puffs was observed along the scan line before wave initiation. Furthermore, the occurrence of these ineffectual events is greatly underestimated in linescan images, since puffs would have occurred throughout the area of the photolysis spot (75 μm radius), but would have been detected only if they arose within ~3 μm either side of the 100-μm long scan line (Yao *et al.*, 1995). The observed

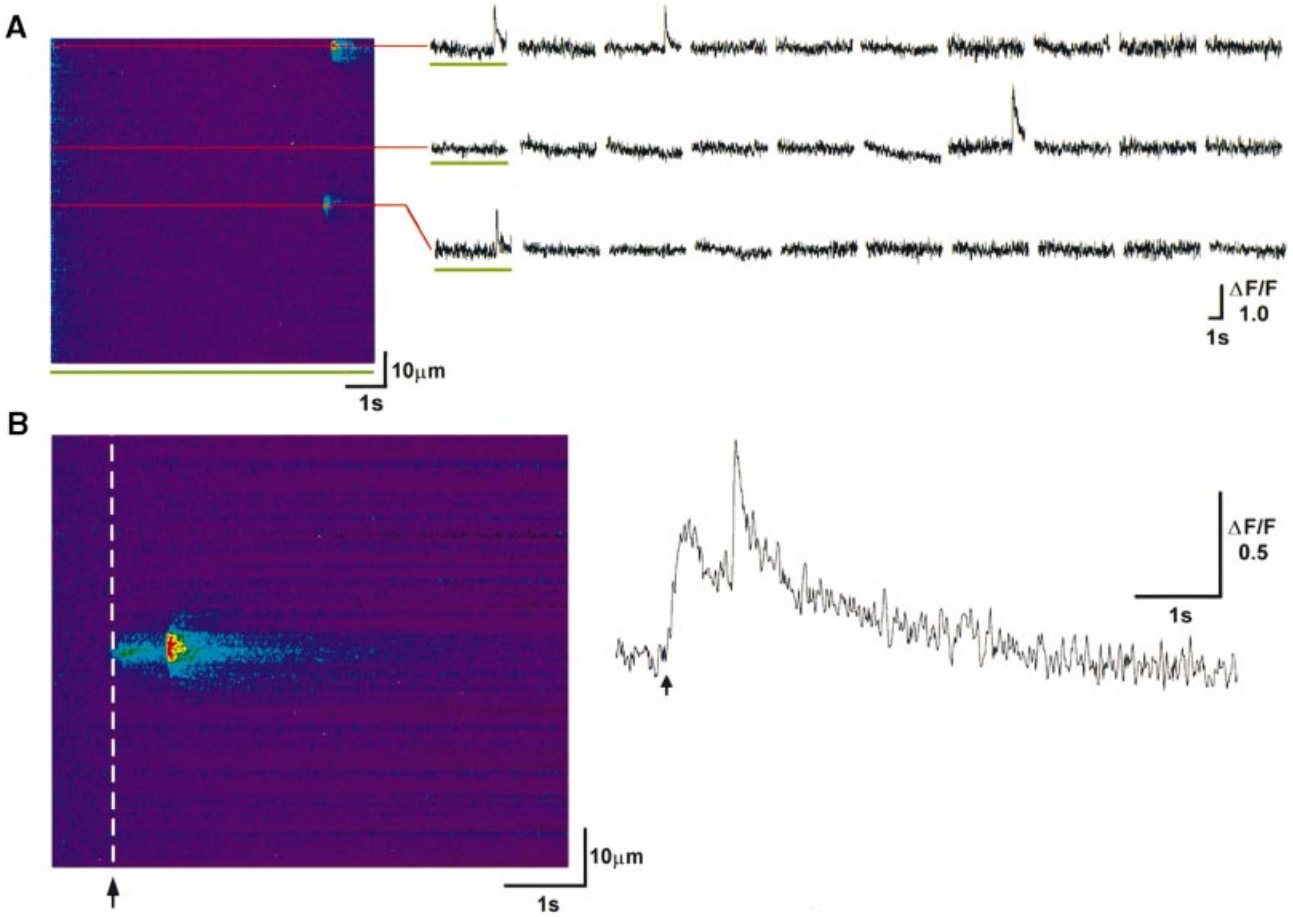

Fig. 5. Ca^{2+} puffs triggered by local Ca^{2+} pulses. (**A**) Representative linescan image of Ca^{2+} puffs evoked by photorelease of IP_3 (flash delivered at the beginning of the record) using an intensity that evoked a low frequency of events. Traces on the right show fluorescence measurements from three sites (marked by red lines in the image), obtained in 10 successive trials. The first traces (underscored in green) were obtained from the illustrated image. (**B**) Linescan image showing a Ca^{2+} transient evoked by laser zap that subsequently evoked a puff. A photolysis flash was delivered at the beginning of the record, using the same flash strength as in (A), and the timing of the laser zap is marked by the dashed line. The puff site corresponds to the lower of the three sites marked in (A). Trace on the right shows fluorescence monitored across a 3-pixel (~0.5 μm) region of the scan line positioned on the center of the laser zap. Timing of the laser zap pulse is marked by the arrow.

events thus represent a restricted sampling within an area of ~600 μm^2, suggesting that as many as 170 puffs could have occurred throughout the entire area of the photolysis spot (75 μm radius = 17 500 μm^2) before a wave initiated. Because a Ca^{2+} wave initiated by any of these events would be observed as it propagated across the scan line, each individual Ca^{2+} puff had a probability of <1% of triggering a wave.

A second observation was that large Ca^{2+} elevations involving concerted release from several adjacent sites were often seen following photorelease of IP_3, but that even these usually failed to trigger waves. Measurements of the signal mass of selected large events that nevertheless failed to trigger waves are plotted in Figure 4B (open bars) for comparison with the puffs. On average these were 3.5 times larger (60.0 s.m.u., n = 130 events) than the mean puff size (17.1 s.m.u., n = 195 events), and events up to 120 s.m.u. sometimes still failed to trigger waves, in agreement with measurements using the UV laser zap technique (Figure 4A).

Triggering of Ca^{2+} puffs by local Ca^{2+} elevations

As demonstrated above, local Ca^{2+} elevations are able to trigger Ca^{2+} waves at concentrations of IP_3 that sufficiently raise the excitability of the cytoplasm, but this process failed if lower concentrations of IP_3 were liberated (Figure 6Ae). We were thus interested to determine whether localized elevations in $[Ca^{2+}]_{cyt}$ could still trigger Ca^{2+} puffs at low concentrations of IP_3, where CICR is thought to be restricted to IP_3 receptors within individual clusters (Bootman and Berridge, 1995; Yao *et al.*, 1995; Parker *et al.*, 1996a). An example of such triggering is shown in Figure 5, where the strength of the photolysis flash was reduced so that no waves, and only infrequent puffs were evoked (mean rate of 0.06 events/s per 100 μm scan line). Puff sites were mapped by imaging responses along a fixed scan line to repeated photolysis flashes (Figure 5A), and the laser zap spot was then positioned close to one of these sites. Local Ca^{2+} elevations evoked by weak [neutral density (ND) >2.5] laser zaps delivered 750 ms after the photolysis flash subsequently triggered Ca^{2+} puffs at the release site in five out of 10 trials (Figure 5B), whereas identical zaps failed to trigger Ca^{2+} liberation when delivered to regions along the scan line that did not show puffs (15 trials). The average signal mass of Ca^{2+} puffs triggered by UV laser-evoked Ca^{2+} pulses (15.6 s.m.u.) was similar to the mean size of spontaneous Ca^{2+} puffs evoked by IP_3 alone. Furthermore,

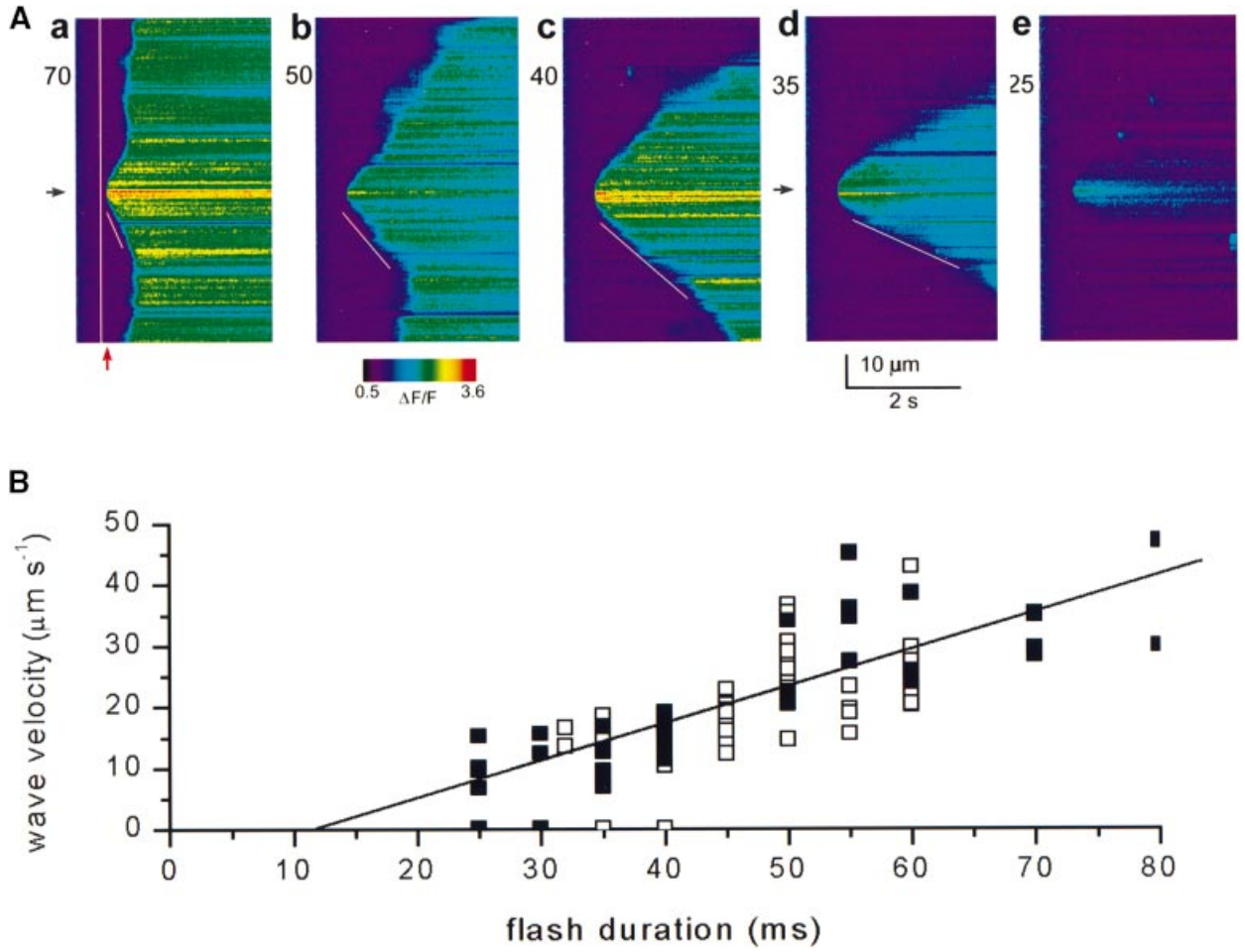

Fig. 6. The velocity of Ca^{2+} waves increases with increasing $[IP_3]$. (**A**) Confocal linescan images show Ca^{2+} waves initiated by laser zap pulses delivered at a fixed interval following photorelease of varying amounts of IP_3. The white vertical line in (a) indicates the timing of the photolysis flash, and the red and black arrows denote, respectively, the timing and position of the UV laser zap spot. The durations of the photolysis flash are indicated in ms next to frames (a–e), and all other parameters remained constant. Measurements of wave velocity were derived from the slopes of lines (indicated in white) fitted by eye to align with the wavefront propagating along the scan line. Following strong flashes (a and b) Ca^{2+} release began spontaneously at multiple sites along the line shortly after a wave was initiated, but it was nevertheless possible to measure wave velocity over a restricted region of the scan. The photolysis flash in (e) was sufficiently weak that the laser zap failed to initiate a wave. (**B**) Measurements derived from images like those in (A) showing the dependence of wave velocity upon duration of the photolysis flash. Data are from the vegetal hemispheres of two oocytes (different symbols), using OG-1 as the indicator.

the average signal mass associated with Ca^{2+} pulses that activated neighboring Ca^{2+} release sites (16.2 s.m.u., ~3.2×10^{-19} mol Ca^{2+}), was similar to the average size of a Ca^{2+} puff (Figure 4B).

Latency to wave initiation does not arise through sensitization to IP_3

The results presented above demonstrate that the oocyte cytoplasm becomes capable of supporting Ca^{2+} waves almost immediately after $[IP_3]$ is elevated, but that Ca^{2+} puffs occurring over the following few seconds are ineffective at triggering waves. To account for the delayed initiation of Ca^{2+} waves we considered two broad possibilities: (i) there is a time-dependent increase in the excitability of the cytoplasm such that a given amount of Ca^{2+} liberated during a puff becomes more effective at triggering a wave; or (ii) there are progressive changes in the amount of Ca^{2+} liberated during a puff so that individual events become more effective triggers for wave initiation (Bootman *et al*., 1997a).

Considering the first of these possibilities, an increased excitability of IP_3 receptors might arise through binding of either IP_3 or Ca^{2+}. To look for changes in IP_3 binding we used measurements of wave velocity as an assay of sensitivity to IP_3. As illustrated in Figure 6A, Ca^{2+} waves initiated by laser zap pulses delivered at a fixed time (100 ms) after photorelease of IP_3 propagated with increasing velocity when the flash duration was lengthened to liberate more IP_3. Furthermore, the wave velocity varied almost linearly with flash duration, increasing from a minimum of ~10 μm/s with just-threshold stimuli to >50 μm/s following strong stimuli (Figure 6B). Despite this strong dependence of wave velocity on $[IP_3]$, however, we found no time-dependent changes in velocity or peak amplitude of waves evoked by laser zaps delivered at varying intervals following photorelease of a fixed amount of IP_3 (Figure 7). These data therefore suggest that the

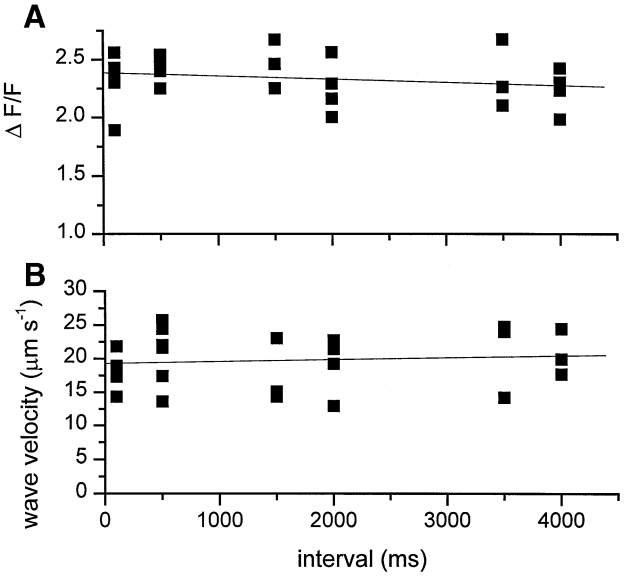

Fig. 7. Ca^{2+} waves triggered by laser zap at varying intervals after photorelease of IP_3 have similar amplitudes and velocities. Measurements were made from records like those in Figure 6C–F, in which Ca^{2+} waves were triggered by a UV laser pulse applied at varying intervals after photolysis flashes of constant strength. (**A**) Peak fluorescence ratio (ΔF/F) of OG-1 during Ca^{2+} waves, plotted against interval between photolysis flash and UV laser zap. Fluorescence was measured across a 3 μm region of the scan line, positioned ~6 μm away from the laser spot on each side of the wave so as to avoid contribution to the signal of Ca^{2+} directly released by the laser zap. Fluorescence ratios (ΔF/F) >3 were sometimes recorded locally at the zap site, indicating that the lower values obtained during waves were not limited by dye saturation. (**B**) Ca^{2+} wave velocity as a function of interval after the photolysis flash. Velocities were measured as illustrated in Figure 6A.

sensitivity to IP_3 does not increase appreciably during the latent period preceding spontaneous wave initiation.

Ca^{2+} puffs do not increase in magnitude before wave initiation

To determine whether a progressive increase in Ca^{2+} puff magnitude might underlie wave initiation, we used a protocol in which paired records were obtained in response to trains of photolysis flashes (3 s intervals) that triggered waves after several seconds (Figure 8B), and to just-subthreshold stimuli (~7% weaker flashes at the same interval) that failed to evoke a wave during a 30 s imaging period in the same oocyte (Figure 8A). The newly available indicator fluo-4 was used for these experiments, as its greater fluorescence change on Ca^{2+} binding enhanced our ability both to detect small events and to resolve small increases in basal $[Ca^{2+}]$ (see below). There was no significant difference in the amount of Ca^{2+} liberated during puffs under conditions where Ca^{2+} waves were or were not initiated: the mean signal mass of all puffs evoked by just-subthreshold stimuli was 16.7 ± 1.2 s.m.u. (n = 745 events, 88 independent trials), as compared with 16.1 ± 2.4 s.m.u. (n = 347 events, 42 independent trials) for puffs that preceded waves evoked by just-suprathreshold stimuli. Furthermore, measurements of peak fluorescence and signal mass of puffs showed no obvious time-dependent changes either with increasing duration of exposure to subthreshold levels of IP_3 (Figure 9A and C), or during the period before waves initiated (Figure 9B and D).

Ca^{2+} puff frequency increases prior to wave initiation

Using the same protocol as described above, we observed marked changes in the frequency with which puffs occurred prior to wave initiation (Figure 8B). The mean interval between successive puffs at a given site shortened from ~5 s soon after beginning photorelease of IP_3 to ~500 ms immediately before waves began (Figure 10B). Furthermore, the numbers of discrete sites generating puffs increased steeply over several seconds before waves initiated (Figure 10C). These changes appeared not to arise primarily as a result of an increasing concentration of IP_3 within the oocyte due to the continuing photostimulation, or to an increasing time of exposure to IP_3, because paired measurements of puff intervals with just-subthreshold stimuli showed no consistent changes throughout the last 20 s of the recording period (Figure 10A). The distributions of inter-puff intervals, pooled from all records with just-subthreshold and just-suprathreshold stimuli, are shown in Figure 10D (open and filled bars, respectively). The mean interval between puffs preceding waves was shorter (2.34 ± 1.07 SD, n = 293 intervals) than that with just-subthreshold stimuli (5.05 ± 1.50 SD, n = 598 intervals), but in both cases the distributions followed similar, skewed patterns.

A further observation from images like that in Figure 8B was that the overall $[Ca^{2+}]$ level became elevated shortly before waves initiated. To quantify this effect and measure its time course, we measured the mean fluorescence across the entire 100 μm scan line, and formed an averaged record by aligning traces from 42 trials to the times at which waves initiated (Figure 11B, gray filled trace). This averaged profile displays a marked elevation in $[Ca^{2+}]_{cyt}$ during the 4 s preceding the abrupt regenerative phase of Ca^{2+} wave initiation (Figure 11B, inset), which corresponds well with the acceleration of Ca^{2+} puff frequency before the wave (Figure 11A). Records obtained in response to just-subthreshold stimuli that failed to evoke waves, on the other hand, showed a smaller and slower elevation of spatially averaged $[Ca^{2+}]_{cyt}$ (Figure 11B, black line).

Discussion

One puff is not enough to initiate a wave

We first examined whether the delayed transition from puffs to waves following a step increase of $[IP_3]$ arose because the cytoplasm was initially incapable of supporting Ca^{2+} wave propagation, by using localized Ca^{2+} elevations evoked using the laser zap technique to probe the excitability of the cytoplasm. Our experiments were done by photoreleasing IP_3 at concentrations that led to spontaneous initiation of waves after several seconds; a situation that mimics physiological activation by moderate doses of Ca^{2+}-mobilizing agonists (Miledi and Parker, 1989; Berridge, 1994; Bootman *et al.*, 1997a), but allows much better temporal and spatial control of cytosolic $[IP_3]$. Ca^{2+} pulses triggered waves as soon as 100 ms after photorelease of IP_3, but the amount of Ca^{2+} required (~2.4×10^{-18} mol of Ca^{2+} for 50% likelihood of triggering

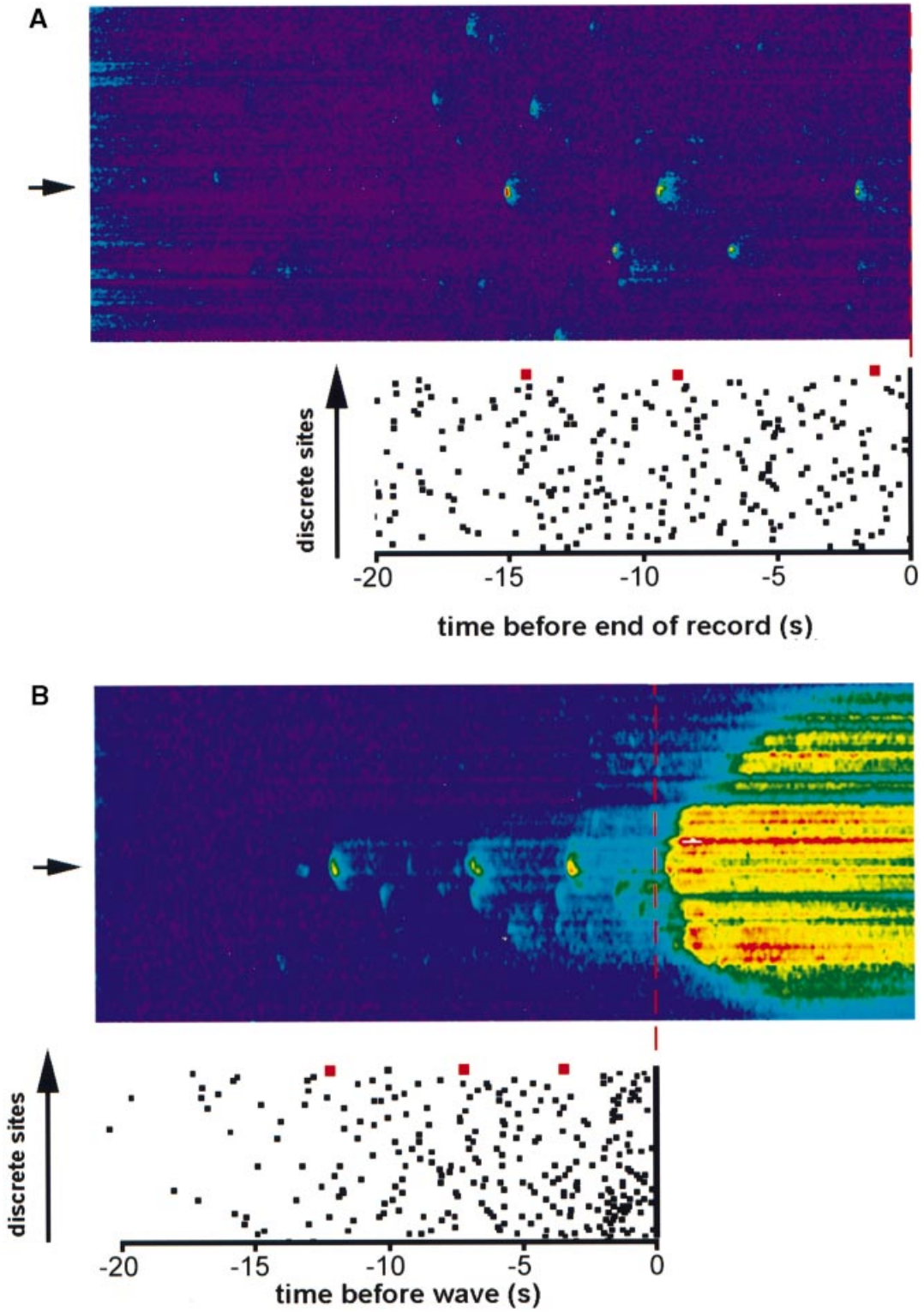

Fig. 8. Patterns of subcellular Ca^{2+} liberation evoked by sustained photorelease of IP_3 at levels just below and just above that required to evoke Ca^{2+} waves. Linescan Ca^{2+} images were obtained as in Figure 3, and show responses to trains of photolysis flashes delivered throughout the records at 3-s intervals. Both frames were obtained from the same 100 μm scan line in the same oocyte, with a flash duration of 36 ms in (**A**) and 40 ms in (**B**). Images were obtained using fluo-4 as the Ca^{2+} indicator. The plots below each linescan image depict the time of occurrence of individual Ca^{2+} puffs arising at discrete sites in >40 scans for each condition (15 oocytes), and represent the dataset used for analysis in Figures 9–11. Data marked by red squares in the top row of each plot correspond to puffs arising at the site marked by arrows in the images. Each subsequent row of symbols similarly represents puffs arising at a discrete site during a single trial.

a wave) was ~7-fold greater than the mean amount liberated during puffs (3.4×10^{-19} mol). Furthermore, numerous puffs and larger localized events occurred during the latent period but failed to trigger waves, and we did not observe any progressive increases in puff magnitude prior to wave initiation. The failure of puffs to evoke

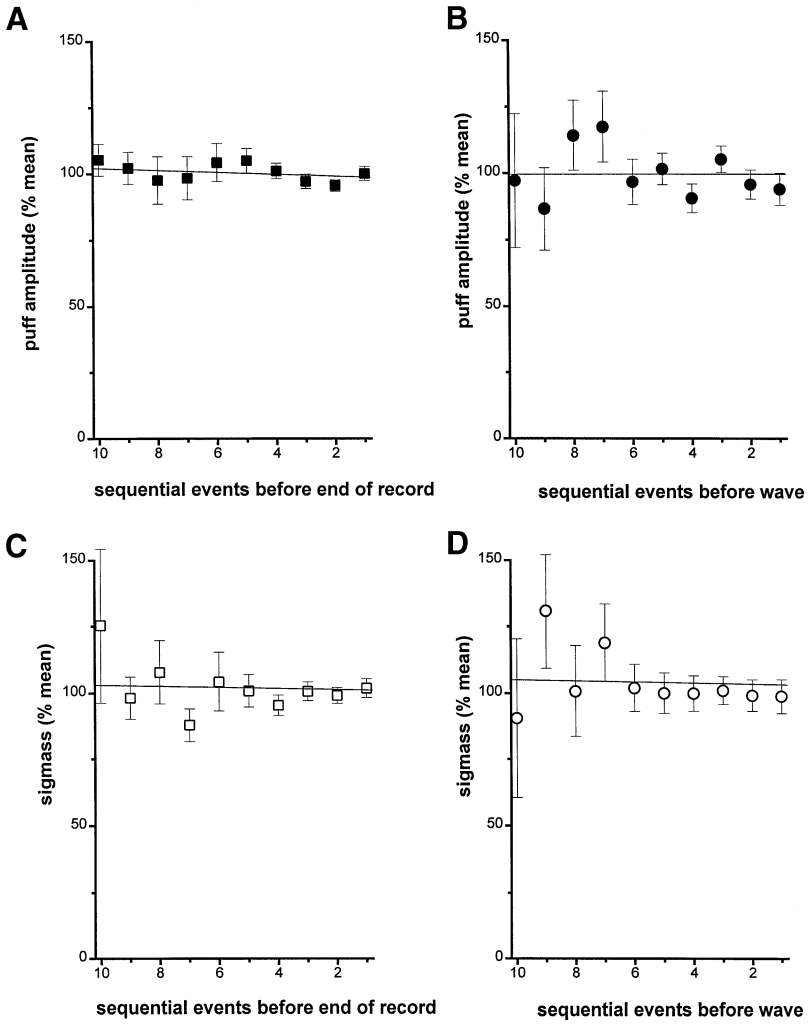

Fig. 9. Puffs do not show time-dependent changes in magnitude prior to wave initiation. Plots show mean measurements in 15 oocytes (five frogs) of the peak local fluorescence change (A, B) and signal mass (C, D) derived from images like those in Figure 8. (**A** and **C**) Data obtained using stimuli (trains of flashes at three intervals) that just failed to evoked waves (n = 745 elementary events, 88 independent sites). (**B** and **D**) Data obtained from the same cells using stimuli that were just-suprathreshold to initiate waves (n = 347 events, 42 independent sites). Measurements were made of repeated puffs arising at given sites, and are plotted after normalizing as a percentage of the mean magnitude of all puffs at that site. Fluorescence ($\Delta F/F$) was monitored from a 0.5 μm wide region of the scan line centered on the puff sites, and signal mass was derived as described in the Materials and methods. The abscissae indicate the order of occurrence of puffs at each site, referenced either to the end of the 30 s record (A, C) or to the time a Ca^{2+} wave began (B, D). Data points show mean ± SEM.

waves soon after elevation of [IP_3] arises, therefore, not because the cytoplasm is inexcitable, but rather because individual puffs are too small to act as effective triggers.

Although individual puffs failed to trigger waves at the concentrations of IP_3 we examined, activation of the same Ca^{2+} release sites was able to support the saltatory calcium wave propagation once a wave was initiated. One explanation is that because Ca^{2+} liberated during an isolated puff diffuses in three dimensions, there is only a modest rise in concentrations at adjacent release sites a few micrometers away. On the other hand, when the same puff site is activated on the edge of a propagating wavefront, the Ca^{2+} concentration is already elevated on either side and behind it by release from other sites, so that the only gradient for net diffusion of Ca^{2+} lies in front of the wave. Release of a given quantity of Ca^{2+} will therefore result in a much higher concentration at an adjacent site immediately ahead of the wave, rendering it more likely to be triggered. Diffusional 'dilution' of Ca^{2+} is minimal for planar waves, but becomes more pronounced for circular waves of progressively smaller radius. Elementary theory of excitable media thus predicts the existence of a critical radius of excitation below which propagation is not possible (Lechleiter *et al.*, 1991) and which, conversely, defines the minimal radius for a Ca^{2+} trigger signal to be effective in initiating a wave. This critical radius, and hence the threshold amount of Ca^{2+} required, depends upon several factors, including the spatial distribution of IP_3 receptors and their sensitization by binding of IP_3 and Ca^{2+} (Bugrim *et al.*, 1997; Keizer *et al.*, 1998).

The generation of Ca^{2+} puffs appears to involve the concerted opening of a few tens of IP_3 receptor/channels, and we have previously proposed that this arises through CICR that remains localized between channels clustered at an individual release site (Parker *et al.*, 1996a; Sun *et al.*, 1998). In support of this interpretation, we demonstrate here that weak laser zap pulses that evoke Ca^{2+} pulses with magnitudes similar to puffs can trigger localized activation of closely adjacent release sites. Ca^{2+}-

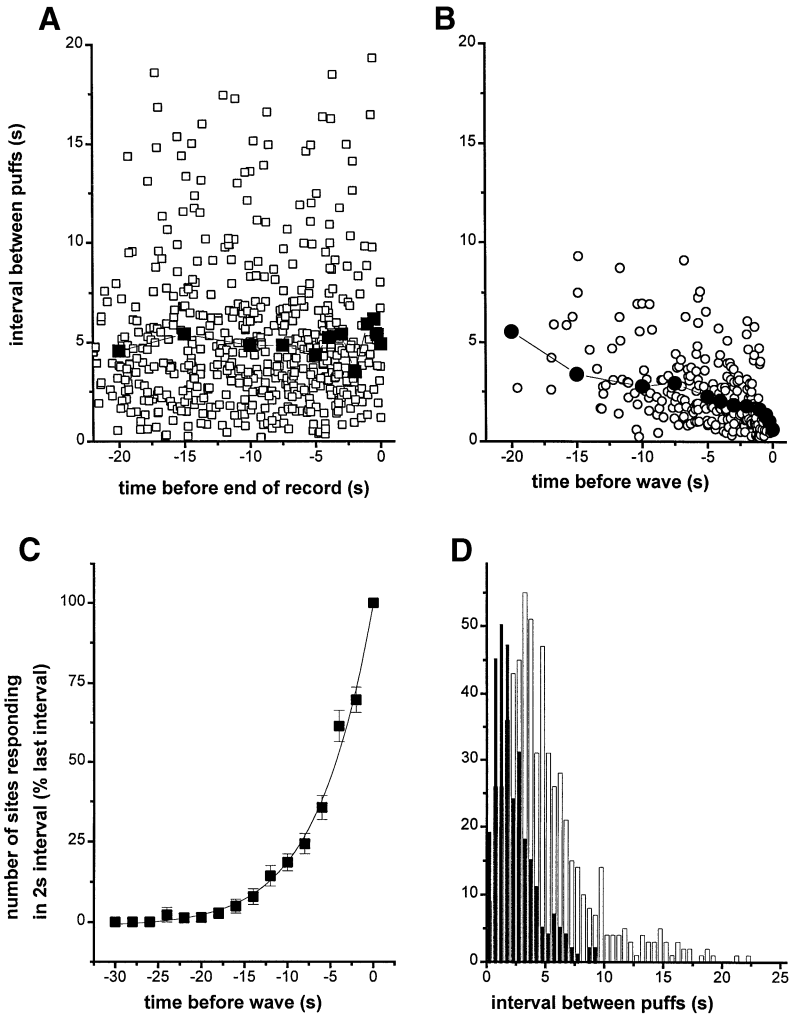

Fig. 10. Puffs arise at increasing frequency prior to wave initiation. (**A** and **B**) Intervals between puffs arising at a given site, plotted as functions of time during the record for sub-threshold stimuli (A), and time before wave initiation for suprathreshold stimuli (B). Open symbols represent measurements from pairs of individual events, and filled symbols show mean intervals averaged over specific time periods. The time 'bins' used for averaging (5000, 2500, 1000, 500 and 250 ms) were selected so as to display better the abrupt shortening in interval preceding wave initiation. (**C**) Increase in the number of calcium release sites generating puffs prior to wave initiation. The ordinate shows mean numbers of sites along the scan line that generated puffs during successive 2-s intervals, scaled as a percentage of the mean number of sites observed in the period immediately preceding wave initiation. (**D**) Histogram showing distributions of puff intervals for all events evoked by just-subthreshold (open bars) and just-suprathreshold stimuli (filled bars).

dependent activation of IP_3 receptors has not been resolved previously at the level of elementary release sites, but our findings are analogous to those of Lipp and Niggli, who observed that localized Ca^{2+} elevations evoked by two-photon photolysis triggered both Ca^{2+} waves and local Ca^{2+} events ('sparks' and 'quarks') mediated by ryanodine receptors in cardiac myocytes (Lipp and Niggli, 1998).

Ca^{2+}-sensitization of IP_3 receptors preceding waves

As noted above, the magnitudes of puffs (peak fluorescence, amount of Ca^{2+} liberated) did not change during the latent period before spontaneous wave initiation, suggesting that waves were triggered because the excitability of neighboring release sites increased sufficiently that puffs of a given size induced CICR, rather than because the puffs grew to become more effective triggers. Because of the co-agonist action of Ca^{2+} and IP_3 at the IP_3 receptor, increased excitability may result from slow binding of IP_3 or from a progressive increase in $[Ca^{2+}]_{cyt}$. We did not observe any time-dependent change in sensitization by IP_3 during the period preceding Ca^{2+} wave initiation, because Ca^{2+} waves triggered at various intervals after photorelease of IP_3 propagated with the same velocity, despite the strong dependence of wave speed on $[IP_3]$. Furthermore, the consistency in magnitudes and frequencies of puffs after photorelease of IP_3 at concentrations below the threshold to evoke waves argues against a slow increase in sensitivity under conditions where the basal $[Ca^{2+}]_{cyt}$ remains steady. Under physiological conditions, submaximal concentrations of IP_3 thus bind to the IP_3 receptor relatively quickly ($<$100 ms), and sensitization of receptors by IP_3 then remains constant prior to Ca^{2+} wave initiation. Although IP_3 receptors in hepatocytes undergo time-dependent inactivation processes consequent to IP_3 binding (Hajnóczky and Thomas, 1994, 1997; Dufour *et al.*, 1997; Marchant and Taylor, 1998), such a regulatory mechanism is either absent from

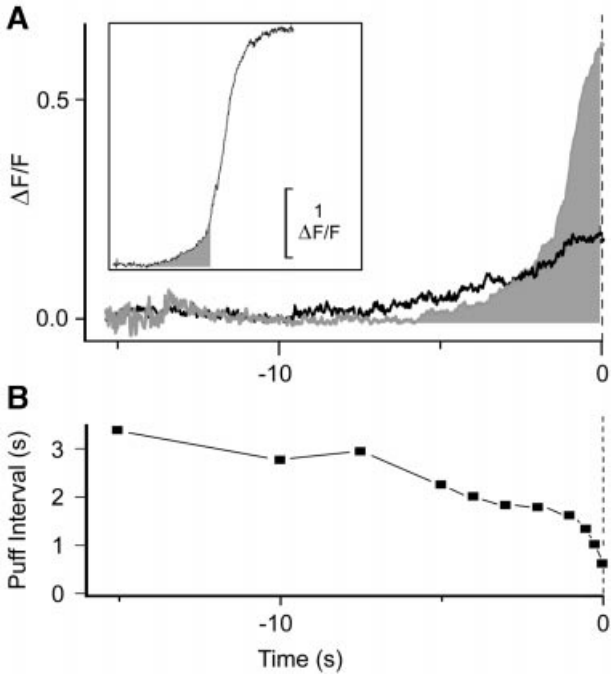

Fig. 11. $[Ca^{2+}]$ increases prior to wave initiation in parallel with increasing puff frequency. (**A**) Main traces show time course of fluo-4 fluorescence across the entire 100 μm laser scan line, averaged from 88 different scan lines where a wave was initiated (filled gray trace) and 44 scan lines with stimuli that were just-subthreshold to evoke a wave (black line). Averages were formed by aligning individual traces to the time of wave initiation or, with subthreshold stimuli, to the end of the 30 s record. Data are from 15 oocytes (five frogs). Inset trace shows, on a reduced vertical scale, an example of a Ca^{2+} wave from a single record. The 'foot' of Ca^{2+} preceding the wave is shaded, and corresponds to the gray trace in the main plot. (**B**) Measurements of mean puff interval as a function of time prior to wave initiation, replotted from Figure 10B.

Xenopus IP_3 receptors at resting $[Ca^{2+}]_{cyt}$ or appears to be kinetically irrelevant over the time-frame of these experiments.

On the other hand, our data revealed two features that probably contribute to the delayed triggering of waves: a marked increase of puff frequency shortly before wave initiation and an abrupt increase in the spatially-averaged $[Ca^{2+}]_{cyt}$. These changes were absent, or much smaller in paired trials where the photorelease of IP_3 was set to be just below threshold to elicit waves, indicating that they did not arise through gradual accumulation of photo-released IP_3. Instead, they probably arose because Ca^{2+} liberated during puffs diffused to cause an elevation of overall $[Ca^{2+}]_{cyt}$. This, in turn, would sensitize release sites, so as to result both in a further increase in frequency of puffs (Yao and Parker, 1994) and in a decrease in the threshold amount of Ca^{2+} required to initiate a wave so that puffs would become more effective triggers. The notion that a subthreshold pacemaker elevation of $[Ca^{2+}]_{cyt}$ precedes regenerative Ca^{2+} waves is not new (Parker and Yao, 1991; Iino and Endo, 1992), but our results further emphasize the roles of elementary release events both in contributing to the pacemaker Ca^{2+} and in providing the final triggering event.

Summation of the 'packets' of Ca^{2+} liberated by puffs to cause a more macroscopic elevation of $[Ca^{2+}]_{cyt}$ will have the effect of reducing the variability resulting from stochastic activity of individual release sites, and may thus account for the relatively constant frequency of Ca^{2+} waves generated at a particular $[IP_3]$ (Yao *et al.*, 1995). This chemical mechanism is thus analogous to the electrical summation of stochastic single-channel openings to provide reproducible macroscopic whole-cell currents. Furthermore, it points to the importance of Ca^{2+} sequestration into the endoplasmic reticulum (Camacho and Lechleiter, 1993) and mitochondria (Jouaville *et al.*, 1995) in determining the integration time for accumulation of $[Ca^{2+}]_{cyt}$ toward a threshold level at which puffs trigger waves.

The mechanisms by which elementary events contribute to global Ca^{2+} signals were previously investigated by Bootman and colleagues in HeLa cells stimulated by an extracellular agonist (Bootman *et al.*, 1997a). They describe how puffs during the pacemaker phase before wave initiation may show increases in amplitude, spatial extent and/or frequency. In the *Xenopus* oocyte, we confirmed the importance of increases in puff frequency, but did not observe any progressive changes in peak amplitude of puffs or in their spatial extent (which would be reflected as an increase in our measurements of signal mass). It is not clear to what extent these differences may arise through differences in cell type, or may be attributed to concomitant changes in $[IP_3]$ resulting from agonist stimulation in the HeLa cells. Nevertheless, we are in agreement with their overall conclusion: that an increasing Ca^{2+} liberation by elementary events drives the ambient $[Ca^{2+}]_{cyt}$ toward a threshold at which a regenerative Ca^{2+} wave is evoked.

Local and global Ca^{2+} signaling

The fact that the amount of Ca^{2+} liberated during puffs is well below the threshold needed to initiate a Ca^{2+} wave allows the oocyte to generate local Ca^{2+} signals that are recruited in a graded manner with increasing stimulation, as well as regenerative global signals. In other cell types the transition between local and global signals may be biased so as to favor one signaling mode or the other, or—as in the oocyte—to allow both modes to coexist. For example, smooth muscle cells utilize both local Ca^{2+} sparks and global Ca^{2+} transients for different functions (Nelson *et al.*, 1995), whereas Ca^{2+} sparks appear to represent the sole physiological signaling mode in cardiac myocytes, and Ca^{2+} waves are apparent only under pathological conditions of Ca^{2+} overload (Cheng *et al.*, 1996). Several factors are important in determining the transition from elementary to global Ca^{2+} transients, including the magnitude and kinetics of Ca^{2+} liberation during each event, the Ca^{2+}-sensitivity of the Ca^{2+} release channels, the spatial organization of release sites, Ca^{2+} sequestration and Ca^{2+} diffusion and buffering within the cytosol. These may be differentially regulated among different cell types, so as to tailor the spatio-temporal patterns of elementary and global calcium signals to serve specific cellular functions.

Materials and methods

Preparation of oocytes and solutions

Experiments were performed on immature oocytes obtained from *Xenopus laevis* as described previously (Callamaras *et al.*, 1998; Sun *et al.*, 1998). Frogs were anesthetized by immersion in a 0.15% aqueous

solution of MS-222 (3-aminobenzoic acid ethyl ester) for 15 min, and small pieces of ovary removed by surgery. Epithelial layers were removed from oocytes either manually or by collagenase treatment (Sigma Type I, used at 1 mg/ml for two consecutive incubations of 1 h). Oocytes were microinjected 1 h prior to recording with fluorescent Ca^{2+} indicator, either alone or together with caged IP_3 [*myo*-inositol 1,4,5-trisphosphate, P4(5)-1-(2-nitrophenyl) ethyl ester], to final intracellular concentrations of ~40 and ~5 μM, respectively. Oregon Green 488 BAPTA-1 (OG-1) was used as the Ca^{2+} indicator for experiments in Figures 2–7, whereas fluo-4 was used in Figures 8–11. This latter indicator became available during the course of our experiments, and provides a greater fluorescence change on binding Ca^{2+}, thus enhancing detection of small increases in [Ca^{2+}]. All recordings were made at room temperature, with oocytes bathed in Ringer's solution (120 mM NaCl, 2 mM KCl, 1.8 mM $CaCl_2$, 5 mM HEPES pH 7.2). Ca^{2+}-free solution was made by omitting $CaCl_2$ and supplementing with 5 mM $MgCl_2$ and 1 mM EGTA. Unless noted, all measurements were obtained in the vegetal hemisphere of pigmented oocytes, bathed in Ringer's solution containing 1.8 mM Ca^{2+}. OG-1, fluo-4 and caged IP_3 were obtained from Molecular Probes Inc. (Eugene, OR). All other reagents were from Sigma Chemical Co. (St Louis, MO)

Confocal Ca^{2+} imaging

Confocal imaging and flash photolysis of caged IP_3 were performed using a custom built optical system constructed around an Olympus IX70 inverted microscope (Parker *et al.*, 1997). In brief, flashes of near-UV light (340–400 nm) were generated using a mercury arc lamp and electronic shutter, while Ca^{2+}-dependent fluorescence signals were monitored along a line formed by repeatedly scanning a spot formed by the focused beam (488 nm) from an argon ion laser. Emitted fluorescence at wavelengths >510 nm was then monitored through a confocal pinhole using an avalanche diode photon counting module. The major modification from the system described previously (Parker *et al.*, 1997) involved the simultaneous use of a focused UV laser spot to cause a transient, localized release of Ca^{2+} in the cytoplasm. Use of this laser zap technique is described in the Results, and Figure 1A illustrates the optical system used to focus pulses from a frequency-tripled (λ = 355 nm) Nd–YAG laser. The oocyte was positioned using the microscope stage to align pigment granules in the vegetal hemisphere with the focus of the UV laser spot. Calculation of the 'signal mass' associated with Ca^{2+} release events was performed using a custom routine (Sun *et al.*, 1998) written in the IDL programming environment (Research Systems Inc., Boulder, CO), which serves to integrate the one-dimensional linescan profile through three dimensions. Only sharp events that appeared to be focal with the laser scan line were selected for processing. The resulting value was scaled in units of $1\Delta F/F \times 10^{-15}$ l, such that one s.m.u. represents a doubling of fluorescence throughout a volume of 1 fl. Previous calibration (Sun *et al*., 1998) indicated that, using OG-1 as the indicator, 1 s.m.u. corresponds to ~2×10^{-20} mol Ca^{2+}. All data are presented as mean ± SEM.

Acknowledgements

This work was supported by the NIH (GM 48071) and by a Wellcome Trust Fellowship (053102) to J.S.M.

References

Adams,S.R., Kao,J.P.Y., Grynkiewicz,G., Minta,A. and Tsien,R.Y. (1988) Biologically useful chelators that release Ca^{2+} upon illumination. *J. Am. Chem. Soc.*, **110**, 3212–3220.

Berridge,M.J. (1994) Relationship between latency and period for 5-hydroxytryptamine-induced membrane responses in the *Calliphora* salivary gland. *Biochem. J.*, **302**, 545–550.

Berridge,M.J. (1997a) The AM and FM of calcium signalling. *Nature*, **386**, 759–760.

Berridge,M.J. (1997b) Elementary and global aspects of calcium signalling. *J. Physiol.*, **499**, 291–306.

Berridge,M.J. and Dupont,G. (1994) Spatial and temporal signalling by calcium. *Curr. Opin. Cell Biol.*, **6**, 267–274.

Berridge,M.J., Bootman,M.D. and Lipp,P. (1998) Calcium—a life and death signal. *Nature*, **395**, 645–648.

Bezprozvanny,I., Watras,J. and Ehrlich,B.E. (1991) Bell-shaped calcium-response curves for Ins(1,4,5)P_3- and calcium-gated channels from endoplasmic reticulum of cerebellum. *Nature*, **351**, 751–754.

Bootman,M.D. and Berridge,M.J. (1995) The elemental principles of calcium signaling. *Cell*, **83**, 675–678.

Bootman,M.D., Berridge,M.J. and Lipp,P. (1997a) Cooking with calcium; the recipes for composing global signals from elementary events. *Cell*, **91**, 367–373.

Bootman,M.D., Niggli,E., Berridge,M.J. and Lipp,P. (1997b) Imaging the hierarchical Ca^{2+} signalling system in HeLa cells. *J. Physiol.*, **499**, 307–314.

Bugrim,A.E., Zhabotinsky,A.M. and Epstein,I.R. (1997) Calcium waves in a model with a random spatially discrete distribution of Ca^{2+} release sites. *Biophys. J.*, **73**, 2897–2906.

Callamaras,N. and Parker,I. (1998) Hemispheric asymmetry of macroscopic and elementary calcium signals mediated by InsP_3 in *Xenopus* oocytes. *J. Physiol.*, **511**, 395–405.

Callamaras,N. and Parker,I. (1999) Radial localization of inositol 1,4,5-trisphosphate-sensitive Ca^{2+} release sites in *Xenopus* oocytes resolved by axial confocal linescan imaging. *J. Gen. Physiol.*, **113**, 199–213.

Callamaras,N., Marchant,J.S., Sun,X.-P. and Parker,I. (1998) Activation and coordination of InsP_3-mediated elementary Ca^{2+} events during global Ca^{2+} signals in *Xenopus* oocytes. *J. Physiol.*, **509**, 81–91.

Camacho,P. and Lechleiter,J.D. (1993) Increased frequency of calcium waves in *Xenopus laevis* oocytes that express a calcium-ATPase. *Science*, **260**, 226–229.

Cheng,H., Lederer,M.R., Lederer,W.J. and Cannell,M.B. (1996) Calcium sparks and [Ca^{2+}]$_i$ waves in cardiac myocytes. *Am. J. Physiol.*, **270**, C148–C159.

Combettes,L., Hannaert-Merah,Z., Coquil,J.-F., Rousseau,C., Claret,M., Swillens,S. and Champeil,P. (1994) Rapid filtration studies of the effect of cytosolic Ca^{2+} on inositol 1,4,5-trisphosphate-induced $^{45}Ca^{2+}$ release from cerebellar microsomes. *J. Biol. Chem.*, **269**, 17561–17571.

Dolmetsch,R.E., Lewis,R.S., Goodnow,C.C. and Healy,J.I. (1997) Differential activation of transcription factors induced by Ca^{2+} response amplitude and duration. *Nature*, **386**, 855–858.

Dufour,J.-F., Arias,I.M. and Turner,T.J. (1997) Inositol 1,4,5-trisphosphate and calcium regulate the calcium channel function of the hepatic inositol 1,4,5-trisphosphate receptor. *J. Biol. Chem.*, **262**, 2675–2681.

Finch,E.A., Turner,T.J. and Goldin,S.M. (1991) Calcium as a coagonist of inositol 1,4,5-trisphosphate-induced calcium release. *Science*, **252**, 443–446.

Gu,X. and Spitzer,N.C. (1995) Distinct aspects of neuronal differentiation encoded by frequency of spontaneous Ca^{2+} transients. *Nature*, **375**, 784–787.

Hagar,R.E., Burgstahler,A.D., Nathanson,M.H. and Ehrlich,B.E. (1998) Type III InsP_3 receptor channel stays open in the presence of increased calcium. *Nature*, **396**, 81–84.

Hajnóczky,G. and Thomas,A.P. (1994) The inositol trisphosphate calcium channel is inactivated by inositol trisphosphate. *Nature*, **370**, 474–477.

Hajnóczky,G. and Thomas,A.P. (1997) Minimal requirements for calcium oscillations driven by the IP_3 receptor. *EMBO J.*, **16**, 3533–3543.

Horne,J.H. and Meyer,T. (1995) Luminal calcium regulates the inositol trisphosphate receptor of rat basophilic leukemia cells at the cytosolic side. *Biochemistry*, **34**, 12738–12746.

Horne,J.H. and Meyer,T. (1997) Elementary calcium-release units induced by inositol trisphosphate. *Science*, **276**, 1690–1693.

Iino,M. (1990) Biphasic Ca^{2+}-dependence of inositol 1,4,5-trisphosphate-incuced Ca^{2+} release in smooth muscle cells of the guinea pig taenia caeci. *J. Gen. Physiol.*, **95**, 1103–1122.

Iino,M. and Endo,M. (1992) Calcium-dependent immediate feedback control of inositol 1,4,5-trisphosphate-induced Ca^{2+} release. *Nature*, **360**, 76–78.

Jouaville,L.S., Ichas,F., Holmuhamedov,E.L., Camacho,P. and Lechleiter, J.D. (1995) Synchronization of calcium waves by mitochondrial substrates in *Xenopus laevis* oocytes. *Nature*, **377**, 438–441.

Kaplan,J.H. and Ellis-Davies,G.C.R. (1988) Photolabile chelators for the rapid photorelease of divalent cations. *Proc. Natl Acad. Sci. USA*, **85**, 6571–6575.

Keizer,J., Smith,G.D., Ponce-Dawson,S. and Pearson,J.E. (1998) Saltatory propagation of Ca^{2+} waves by Ca^{2+} sparks. *Biophys. J.*, **75**, 595–600.

Lechleiter,J.D., Girard,S., Peralta,E. and Clapham,D. (1991) Spiral calcium wave propagation and annihilation in *Xenopus laevis* oocytes. *Science*, **252**, 123–126.

Li,W.H., Llopis,J., Whitney,M., Zlokarnik,G. and Tsien,R.Y. (1998) Cell-permeant caged InsP_3 ester shows that Ca^{2+} spike frequency can optimize gene expression. *Nature*, **392**, 936–941.

Lipp,P. and Niggli,E. (1998) Fundamental calcium release events revealed by two-photon excitation photolysis of caged calcium in guinea-pig cardiac myocytes. *J. Physiol.*, **508**, 801–809.

Marchant,J.S. and Taylor,C.W. (1997) Cooperative activation of inositol trisphosphate receptors by sequential binding of IP_3 and Ca^{2+} safeguards against spontaneous activity. *Curr. Biol.*, **7**, 510–518.

Marchant,J.S. and Taylor,C.W. (1998) Rapid activation and partial inactivation of inositol trisphosphate receptors by inositol trisphosphate. *Biochemistry*, **37**, 11524–11533.

Marshall,I.C.B. and Taylor,C.W. (1993) Biphasic effects of cytosolic calcium on Ins(1,4,5)P_3-stimulated Ca^{2+} mobilization in hepatocytes. *J. Biol. Chem.*, **268**, 13214–13220.

Meyer,T., Wensel,T. and Stryer,L. (1990) Kinetics of calcium channel opening by inositol 1,4,5-trisphosphate. *Biochemistry*, **29**, 32–37.

Miledi,R. and Parker,I. (1989) Latencies of membrane currents evoked in *Xenopus* oocytes by receptor activation, inositol trisphosphate and calcium. *J. Physiol.*, **415**, 189–210.

Nelson,M.T., Cheng,H., Rubart,M., Santana,L.F., Bonev,A., Knot,H. and Lederer,W.J. (1995) Relaxation of arterial smooth muscle by calcium sparks. *Science*, **270**, 633–637.

Parker,I. and Ivorra,I. (1990) Inhibition by Ca^{2+} of inositol trisphosphate-mediated Ca^{2+} liberation: a possible mechanism for oscillatory release of Ca^{2+}. *Proc. Natl Acad. Sci. USA*, **87**, 260–264.

Parker,I. and Yao,Y. (1991) Regenerative release of calcium from functionally discrete subcellular stores by inositol trisphosphate. *Proc. R. Soc. Lond. B*, **246**, 269–274.

Parker,I., Choi,J. and Yao,Y. (1996a) Elementary events of InsP_3-induced Ca^{2+} liberation in *Xenopus* oocytes: hot spots, puffs and blips. *Cell Calcium*, **20**, 105–121.

Parker,I., Yao,Y. and Ilyin,V. (1996b) Fast kinetics of calcium liberation induced in *Xenopus* oocytes by photoreleased inositol trisphosphate. *Biophys. J.*, **70**, 222–237.

Parker,I., Callamaras,N. and Wier,W.G. (1997) A high-resolution, confocal laser-scanning microscope and flash photolysis system for physiological studies. *Cell Calcium*, **21**, 441–452.

Ramos-Franco,J., Fill,M. and Mignery,G.A. (1998) Isoform-specific function of single inositol 1,4,5-trisphosphate receptor channels. *Biophys. J.*, **75**, 834–839.

Rizzuto,R., Brini,M., Murgia,M. and Pozzan,T. (1993) Microdomains with high Ca^{2+} close to IP_3-sensitive channels that are sensed by neighbouring mitochondria. *Science*, **262**, 744–747.

Sun,X.-P., Callamaras,N., Marchant,J.S. and Parker,I. (1998) A continuum of InsP_3-mediated elementary Ca^{2+} signalling events in *Xenopus* oocytes. *J. Physiol.*, **509**, 67–80.

Thomas,A.P., Bird,G.St J., Hajnóczky,G., Robb-Gaspers,L.D. and Putney,J.W.,Jr (1996) Spatial and temporal aspects of cellular calcium signalling. *FASEB J.*, **10**, 1505–1517.

Thorn,P. (1996) Spatial domains of Ca^{2+} signaling in secretory epithelial cells. *Cell Calcium*, **20**, 203–214.

Walker,J.W., Somlyo,A.V., Goldman,Y.E., Somlyo,A.P. and Trentham, D.R. (1987) Kinetics of smooth and skeletal muscle activation by laser pulse photolysis of caged inositol 1,4,5-trisphosphate. *Nature*, **327**, 249–252.

Yao,Y., Choi,J. and Parker,I. (1995) Quantal puffs of intracelluler Ca^{2+} evoked by inositol trisphosphate in *Xenopus* oocytes. *J. Physiol.*, **482**, 533–553.

Received June 24, 1999; revised July 29, 1999; accepted August 5, 1999